



SIMULATION ANALYSIS OF SHAKING TABLE TEST FOR RC SEISMIC SHEAR WALL IN MULTI-AXIS LOADING TESTS

**Koichi YABUCHI¹, Hiroshi MORIKAWA², Atsushi SUZUKI³,
Yoshio KITADA⁴, Shinsuke OGURI⁵, Katsuki TAKIGUCHI⁶**

SUMMARY

Nuclear Power Engineering Corporation (NUPEC) conducted a shaking table test for reinforced concrete seismic shear wall using the shaking table of Public Works Research Institute of Japan as for a part of the project of 'Model Tests of Multi-Axis Loading on RC Shear Walls'. The shapes of the specimens are box type wall and cylindrical wall. The dimensions of the box type RC shear wall are 1.5m by 1.5m in plan and 1.0m in height. The dimensions of the cylindrical shear wall are 1.9m in diameter and 1.0m in height. The tests were performed by applying two horizontal motions (X, Y) and vertical motion (Z) simultaneously. The tests consist of eight or nine step testing. In each step, the applied accelerations are increased step by steps. Every wall face of each specimen reached failure simultaneously in the final excitation step.

In this paper, results of three-dimensional FEM analyses which simulate test results are discussed. A shear wall were modelled four-node layered shell elements considering out-of-plane shear deformation. The upper slab, base slab and added weight were modelled with shell elements. Four-direction crack model is used with two orthogonal coordinates corresponding to non-orthogonal cracks. NUPEC model developed by the Element Test in 'Model Tests of Multi-Axis Loading on RC Shear Walls' was used for shear transfer mechanism along shear crack surface. Material properties of concrete were derived from material test results conducted at the test day. Damping factor was estimated from the test results.

INTRODUCTION

NUPEC carried out a test project focused on multi-axes loading of RC shear walls, which is entitled 'Model Tests of Multi-Axis Loading on RC Shear Walls' and is sponsored by Ministry of Economy, Trade and Industry of Japan (METI). Dynamic tests using a shaking table of Public Works Research Institute in Japan were conducted, as a part of the test project. Specimen, test condition and test results are described

¹ Kajima Corporation, Tokyo, JAPAN, E-mail: coyabu@kajima.com

² Kajima Corporation, Tokyo, JAPAN, E-mail: morihiro@kajima.com

³ Kajima Corporation, Tokyo, JAPAN, E-mail: a-suzuki@kajima.com

⁴ Japan Nuclear Energy Safety Organization, Tokyo, JAPAN, E-mail: kitada-yoshio@jnes.go.jp

⁵ Japan Nuclear Energy Safety Organization, Tokyo, JAPAN, E-mail: oguri-shinsuke@jnes.go.jp

⁶ Tokyo Institute of Technology, Tokyo, JAPAN, E-mail: ktakiguc@tm.mei.titech.ac.jp

in other papers [1][2]. Japan Nuclear Energy Safety Organization (JNES) succeeded to the project on October 2003 and evaluated the test results.

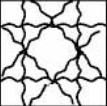
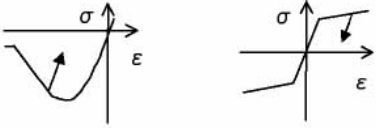
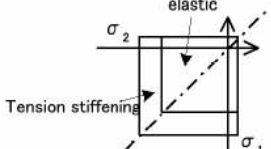
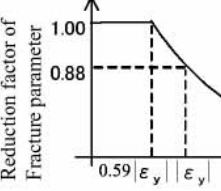
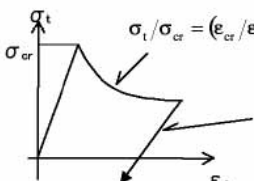
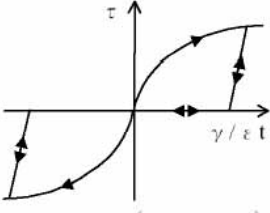
In this paper, simulation analyses of the test results with simultaneous 3-direction input motions by three dimensional nonlinear finite element analysis (3D-FEM) are presented and discussed. Since this detailed analysis model had a large number of degrees of freedom, computing time for calculation tends to be enormous in the case of dynamic response analysis with many steps compared to static response analysis. However, the shape and the structural conditions of the specimen can be modelled and 3D-FEM made it possible to study failure process and to evaluate cracks distribution in detail. With such reasons, this analysis method is thought to be effective for the simulation of these test results.

ANALYSIS CONDITION

Analysis program for simulation

As shown in the test results [1][2], both diagonal shear cracks and horizontal bending cracks are observed on each face of the shear wall according to simultaneous horizontal two directional input. In order to simulate such failure mode, FEM analysis program should have a function to deal with at least three directional cracks in finite elements. Moreover, shear wall is needed to be evaluated three dimensional coordinates using laminated shell elements to consider out-of-plane component. In this study, analysis program considering laminated shell elements to evaluate non-orthogonal 4-directional cracks and out-of-plane components, as shown in Table 1. Condition to generate the non-orthogonal cracks is that intersection angle between the cracks is more than 15 degree. In the case that the angle is less than 15 degree, the cracks are regarded as a single crack.

Table1. Summary of analysis program

| items | contents |
|---|---|
| Element | 4-node laminated shell element taking out-of-plane shear deformation into consideration |
| Cracking model of concrete |  <p>- 4-direction crack installing 2 orthogonal coordinates corresponding to nonorthogonal 2-direction cracks -calculate concrete stress in the coordinates corresponding to active cracks by Fukuura and Maekawa</p> |
| Stress strain relationship |  <p>Concrete (Fafitis & Shah's equation) Rebar(Filippou model)</p> |
| Condition of yielding and fracture | <p>Orthogonal anisotropic model by Hayami and Miyashita</p>  |
| Stiffness reduction and strength reduction ratios post cracking |  <p>$\beta = \frac{1}{0.80 + 0.34 \left \frac{\epsilon_{dt}}{\epsilon_y} \right }$</p> <p>•• Vecchio and Collins ϵ_y: Compressive strain at concrete strength</p> |
| Adherence between concrete and rebars | Completely adherence |
| Tensile characteristics |  <p>$\sigma_t / \sigma_{cr} = (\epsilon_{cr} / \epsilon_t)^c$. Skeleton curve by Izumo (where, $c=0.2 \sim 0.4$) $E_{TR} = E_0 (\epsilon_{cr} / \epsilon_t)^d$ by Tamai's equation (where, $d=0.75 \sim 1.0$)</p> |
| Shear transferring model at crack surface |  <p>-Element test results by NUPEC -hysteresis loop by Maekawa</p> <p>τ: Shear stress γ: Shear strain ϵ_t: Tensile strain</p> $\frac{d\tau}{d\gamma} = \log \left(\frac{85G_0}{\sqrt{\gamma^2 + 0.06 \cdot \epsilon_t^2}} \right)$ |

Analysis condition

Material properties

Material properties of concrete and rebar are determined according to material strength test results. The splitting tensile strength with reduction factor is used as for the tensile strength of concrete [2]. As for damping factor, inertial viscous damping proportional to initial stiffness is used as 3% or 1% at 1st natural frequency. Table 2 shows the material properties used for the analysis.

Table 2 Material properties

| Specimen | Box type wall | Cylindrical wall | |
|--|------------------------------------|------------------|------------|
| Concrete of Wall *1 (equal to upper slab) | Young's modulus | 26.6 GPa | 30.7 GPa |
| | Compressive strength | 34.4 MPa | 37.5 MPa |
| | Strain at the compressive strength | 2207 μ | 1928 μ |
| | Poisson's ratio | 0.190 | 0.161 |
| | Tensile strength*2 | 1.31 MPa | 1.636 MPa |
| | Damping factor | 3% or 1% | 3% or 1% |
| Rebar (D6) *3 | Young's modulus | 180 GPa | 185 GPa |
| | Yield strength | 376 MPa | 377 MPa |
| | Tensile strength | 479 MPa | 491 MPa |

*1 Material tests for concrete test pieces were carried out during excitation test.

*2 Tensile strength of concrete is estimated considering splitting test results with reduction factor.

*3 Based on material tests for pieces.

Analysis model

Three dimensional finite element models were used for the simulation analysis as shown in Figure 1. The wall, upper slab and attached mass were modelled with laminated shell element (eight layered) is applied for all the elements. The boundary was fixed conditions at the bottom of the wall.

Since rotational response motion is observed at the upper slab in the test results, the upper slab of the analysis model has the geometry of the actual upper slab and attached weight. The mass of the slab and attached weight is distributed at all the contact points so that rotational inertia is the same as the specimen. Reinforcement ratio of the specimen is 1.2% at each side in each direction. In the analysis model, a steel layer corresponding to rebar ratio is considered among concrete layers as the shell elements.

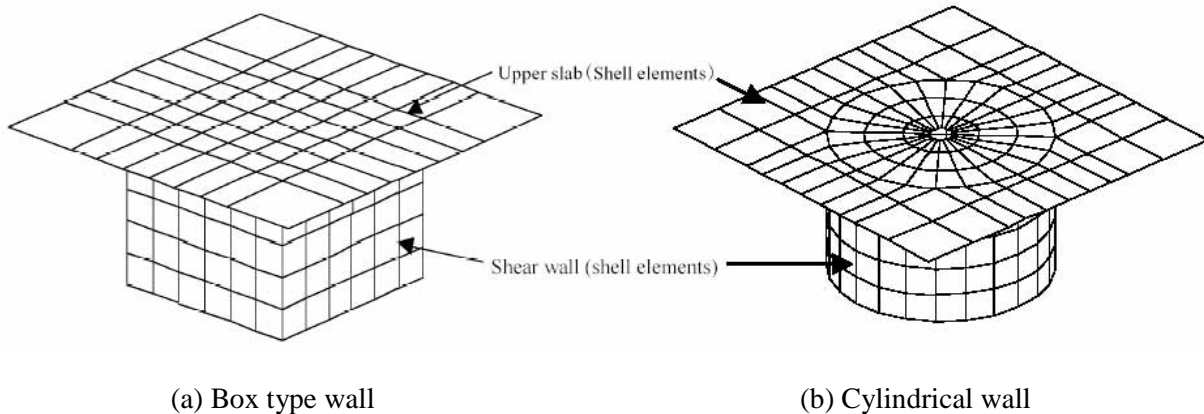


Figure 1 Analysis model

Input motion

Input motion used for the analysis is response acceleration time history observed at the top of the base mat slab. Two horizontal and vertical components are employed simultaneously at the bottom of the wall of the analysis model. Low pass filter is used to cut high frequency components more than 60Hz.

Analysis case

Analysis cases are shown in Table 3 and Table 4. Analyses from case B1 to case B5 are performed for box type wall. Analyses of case C1 and case C2 are for cylindrical wall.

In case B1, simulation analysis of RUN-1 is performed. Main purpose of this analysis case is to verify the modelling method for the wall and upper slab. The excitation control relatively works well during RUN-1 excitation, the achieved motion at the base mat slab is similar to target motion. Natural frequency of the specimen is hardly changed. Neither failure nor cracks at the box wall are observed. In this excitation, the response of the specimen still remains in elastic state.

In case B2, simulation analysis of RUN-2 is performed. Main purpose of this analysis case is to evaluate nonlinear behaviour, such as acceleration and deformation response, also failure mode like crack pattern. During the excitation RUN-2, the natural frequency of the specimen shifts from 22Hz to 15Hz. Thin shear cracks and bending cracks are observed at the wall surface.

In case B3, simulation analysis with continuous input motion of RUN-3, RUN-3' and RUN-4 is performed. Main purpose of this analysis case is to evaluate nonlinear behaviour, such as acceleration response and failure mode under relatively large input motion. The target excitations in this case are RUN-3' and RUN-4, which make the failure of the specimen progress. In the continuous analysis, it is ideal to input every continuous motion before test applies. However to perform these kind of analysis takes enormous computing time. Therefore, continuous motion which consists of target motions and one motion of just before target motions is used for convenience, and it makes the wall elements of the model fail to some extent before target motions start.

In case B4, simulation analysis with continuous input motion of RUN-5, RUN-6 and RUN-7 is performed. Main purpose of the analysis case is to perform evaluation of structural failure. The target excitations in this case are RUN-6 and RUN-7, which make the specimen fail at the bottom of the wall.

In case B5, simulation analysis with 1% damping factor is performed. Input motion and the target excitation is the same condition as case B4. Main purpose of the analysis case is to evaluate effect of damping factor

In case C1, simulation analysis with continuous input motion of RUN-1 through RUN-5' is performed. The damping factor is used as 3%. Main purpose of the analysis case is to perform evaluation of difference between box type wall and cylindrical wall.

In case C2, simulation analysis with 1% damping factor is performed. Main purpose of the analysis case is to evaluate effect of damping factor for cylindrical wall.

Table 3 Analysis case (box type wall)

| Analysis Case | Excitant Steps | | | | | | | | | Damping factor | Notes |
|---------------|----------------|--------|---------|--------|---------|--------|--------|--------|--------|----------------|---|
| | RUN -1 | RUN -2 | RUN -2' | RUN -3 | RUN -3' | RUN -4 | RUN -5 | RUN -6 | RUN -7 | | |
| Case B1 | • | | | | | | | | | 3% | |
| Case B2 | | • | | | | | | | | 3% | |
| Case B3 | | | | | • | • | | | | 3% | Input 3 Steps (RUN-3 + RUN-3' + RUN-4) |
| Case B4 | | | | | | | | • | • | 3% | Input 3 Steps (RUN-5 + RUN-6 + RUN-7) |
| Case B5 | | | | | | | | • | • | 1% | Input 3 Steps (RUN-5 + RUN-6 + RUN-7) |

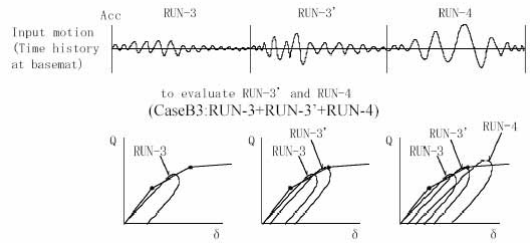


Figure 2 Input motion of continuous analysis

Table 4 Analysis case (cylindrical wall)

| Analysis Case | Excitant Steps | | | | | Damping factor | Notes |
|---------------|----------------|--------|---------|--------|--------|----------------|--------------------------------------|
| | RUN -4 | RUN -5 | RUN -5' | RUN -6 | RUN -7 | | |
| Case C1 | • | • | • | | | 3% | Input 7 Steps (RUN-1 to RUN-5') |
| Case C2 | | | | • | • | 1% | Input 9 Steps (RUN-1 to RUN-7) |

THE ANALYSIS RESULT

Case B1 (RUN-1, elastic response)

Horizontal and vertical natural frequencies of the analysis model are 22.8Hz and 44.9Hz, respectively. These values are almost same values as test results obtained in small input level shaking, which is conducted to confirm the initial condition of the specimen before RUN-1 excitation.

In RUN-1 excitation analysis, all elements keep elastic state. Response acceleration time history of the upper slab and time history of relative displacement between upper slab and base mat slab (displacement, hereafter), both analysis and test results are shown in Figure 3 and 4, respectively.

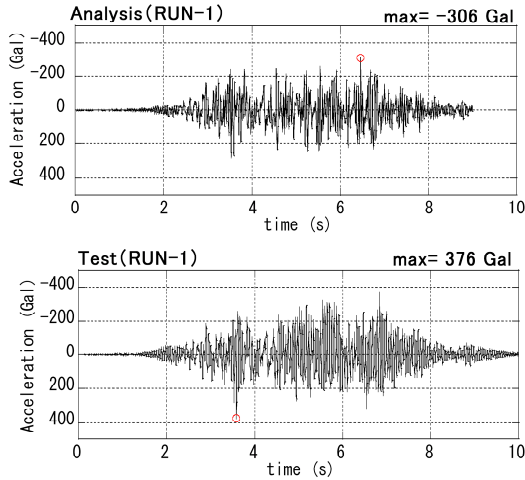


Figure 3 Acceleration time history (Y-direction)

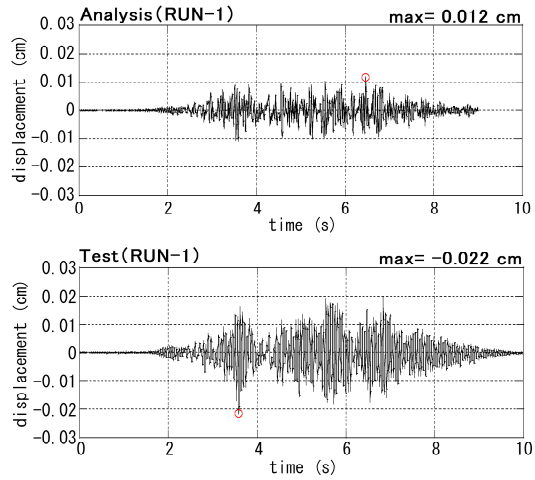


Figure 4 Displacement time history (Y-direction)

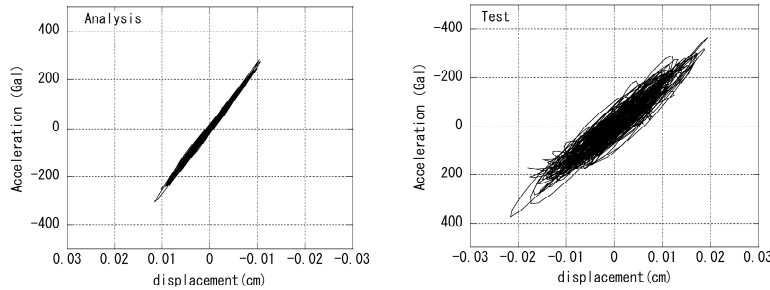


Figure 5 Hysteresis loop (CaseB1, Y-direction)

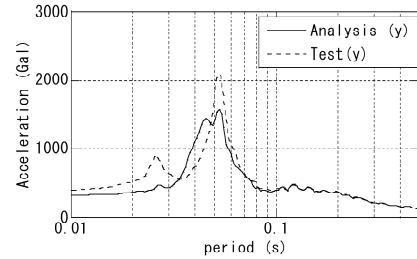


Figure 6 Response spectra (CaseB1, Y-direction)

Response acceleration and response displacement of analysis results are smaller than those of the test results, however, in relatively small amplitude, test result and analysis result are corresponding each other. Figure 5 shows the comparison of hysteresis loop between analysis and test results. According to those comparisons, the stiffness of analysis model is thought to be little larger than that of the test.

Figure 6 shows comparison of acceleration response spectra at the upper slab. Dominant period of the test result is around 0.05s, otherwise that of analysis result is around 0.05s to 0.04s. Two peaks are shown in the analysis results. That is because input motion that is observed during excitation includes dynamic characteristics of the actual specimen. In order to simulate test results more accurately, dynamic characteristics of analysis model needs to be corresponding to that of actual specimen including boundary conditions.

Case B2 (RUN-2, nonlinear response)

Initial condition of the specimen before excitation RUN-2 is elastic state, therefore, initial condition of analysis model is also elastic. Figure 7 and Figure 8 show comparisons of horizontal and vertical acceleration time history of RUN-2, both analysis and test results, respectively. In the initiation of excitation (up to 3s), acceleration of analysis shows a good agreement with test results in horizontal and vertical direction. After 3s when the horizontal dynamic characteristic is remarkably changed, acceleration amplitude of analysis results in horizontal direction is larger than that of test results. Vertical acceleration of analysis is well simulated. In compared with horizontal response, change of vertical dynamic characteristics is relatively small during the excitation.

Figure 9 shows horizontal (Y-direction) displacement time history. Displacement of analysis results is relatively good agreement with that of test results.

Figure 10 shows comparison of hysteresis loop up to 3s. Initial stiffness and acceleration amplitude of analysis model show good agreement with those of test results. Figure 11 shows comparison of hysteresis loop post 3s. During major excitation period, analysis results show larger acceleration amplitude compared to test result.

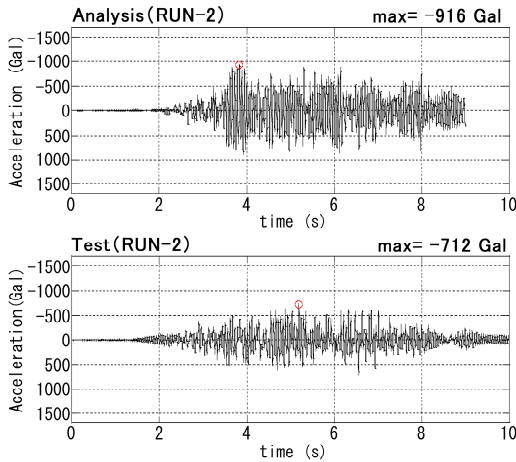


Figure 7 Acceleration time history(Y-direction)

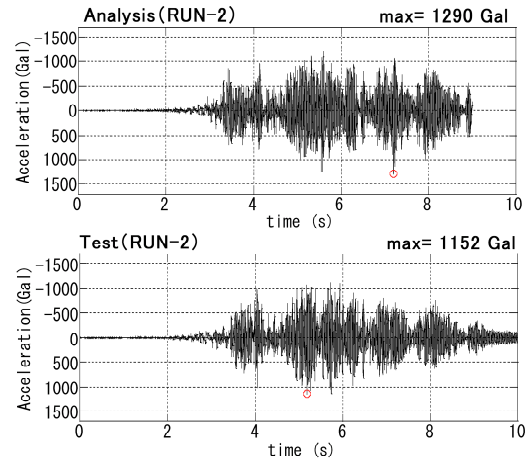


Figure 8 Acceleration time history(Vertical-direction)

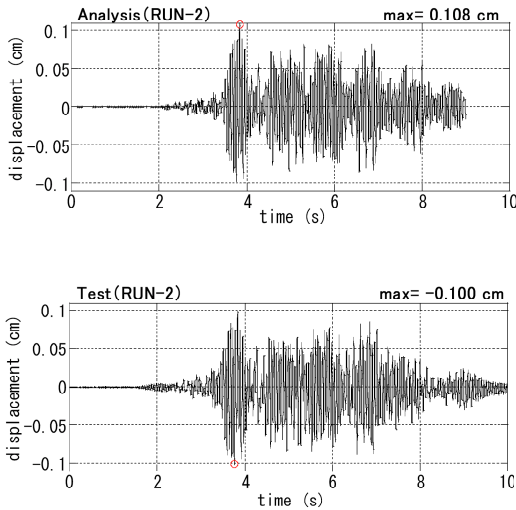


Figure 9 Displacement time history(Y-direction)

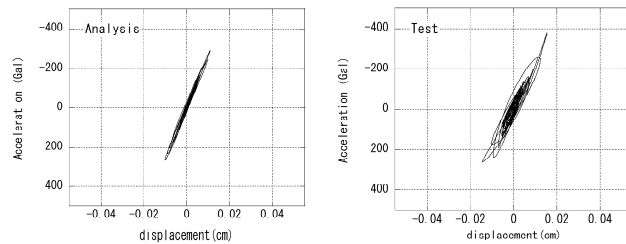


Figure 10 Hysteresis loop(Case B2, 0s-3s, Y-direction)

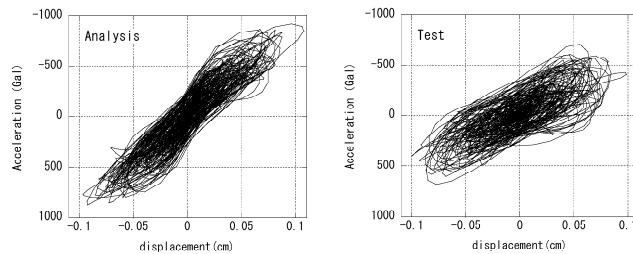


Figure 11 Hysteresis loop(Case B2, 3s-10s, Y-direction)

Figure 12 shows comparison of crack pattern between test results and analysis results. Active and dormant cracks beyond 1000μ are shown in analysis result. Black line and grey line show the active crack and the dormant crack, respectively. Analysis results give good agreement in the crack patterns with those of test results. Difference of damages on each surface of the walls and orientations of cracks are relatively well simulated by the analysis.

Figure 13 shows shift of dynamic characteristics of specimen in RUN-2. Upper part of the figures show running Fourier spectra ratio of acceleration response of upper slab by that of base mat slab. Lower part of the figures show acceleration time history of base mat slab. This figure shows that dynamic

characteristics of the specimen shifts during the RUN-2 excitation. These white zones of the upper figure show natural frequency. It is important to simulate the shift as the change of nominal frequency of the specimen in this analysis case. In the analysis results, the tendency of reduction of nominal frequency during the excitation is shown.

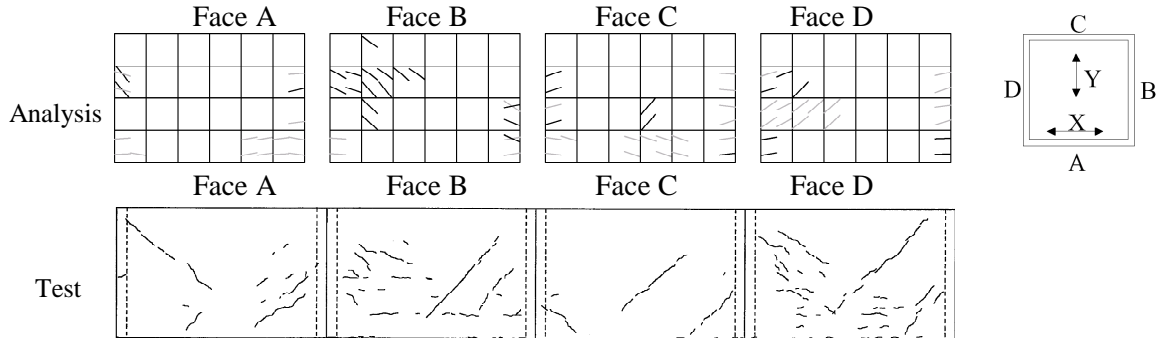


Figure 12 Crack pattern (Case B2)

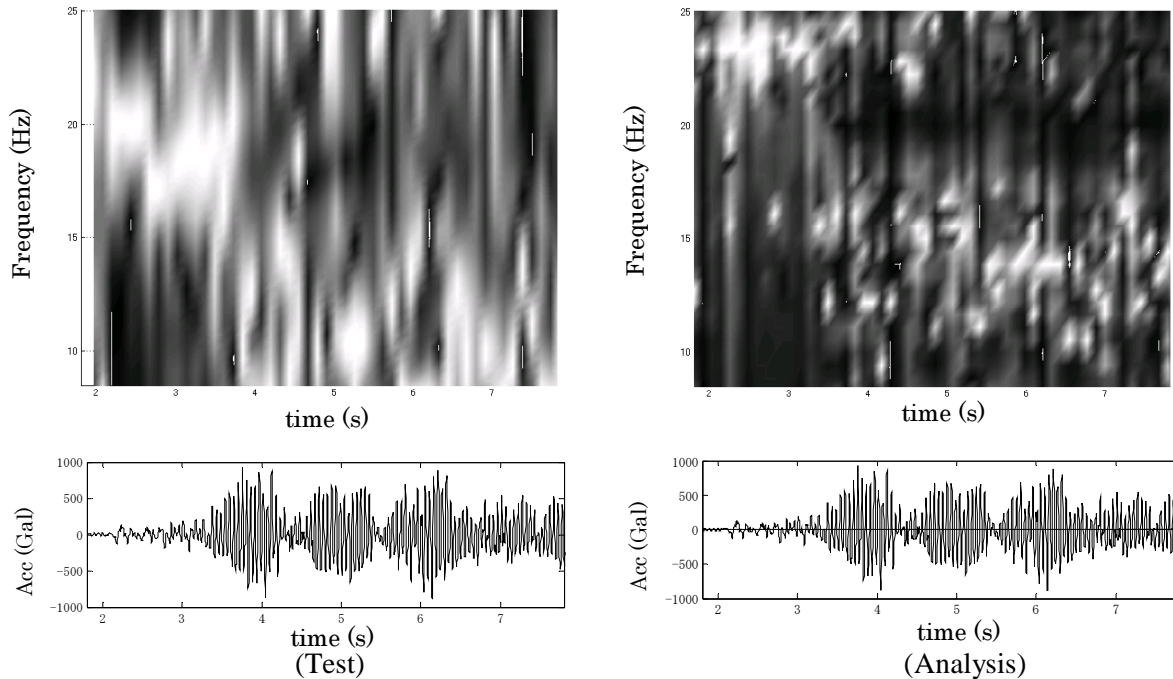


Figure 13 Shift of dynamic characteristics of specimen (RUN-2)

Equivalent viscous damping factor of the specimen is estimated as 4% to 5% during RUN-2 excitation from hysteresis loop (load-deflection relationship) of the test results. According to these results, inertial viscous damping factor of the analysis model is determined as 3% at initial condition. In order to validate this analysis condition, equivalent viscous damping factor is evaluated from hysteresis loop of analysis results in same manner as the evaluation of test results. Figure 14 shows evaluated damping factor from analysis results of 1 second excitation period of 7.5s to 8.5s of analysis results which is supposed to include less plastic damping. Upper figure shows the evaluated damping factor. Horizontal axis shows maximum deformation of the hysteresis loop for calculation, vertical axis shows the damping factor. Blue mark shows calculated value, Red line shows averaged value. It seems that the equivalent damping factors in the analysis case are about 3 to 5%, which is corresponding to those from test.

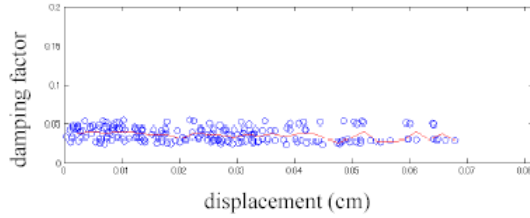


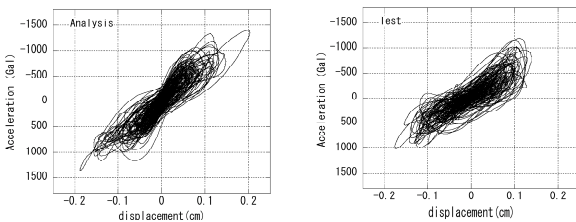
Figure 14 Equivalent viscous damping (RUN-2)

Case B3, Case B4 (large amplitude excitation)

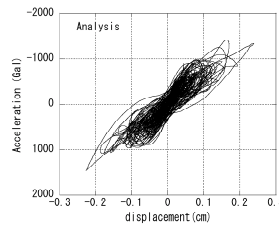
Figure 15 and 16 show comparison of hysteresis loops in Case B3 (RUN-3' and RUN-4). On the RUN-3' excitation, maximum acceleration and horizontal (X-direction) deflection reach 1200 Gal and 0.17cm(1.7/1000 rad), respectively. Hysteresis loop shows S-shape which is typical feature in case of strong nonlinearity of RC wall. Acceleration and deflection of analysis results show a little larger than those of test results. It seems that hysteresis loop of analysis results is S-shape as observed in test results.

Figure 17 and 18 show crack patterns in Case B3 (RUN-3' and RUN-4). Active and dormant cracks beyond 1500 μ are shown in analysis result. Crack pattern on the wall in the analysis shows a good agreement with test results in its generating feature; shear cracks in Face A and Face C corresponding web wall in X direction are generated remarkably, flexural cracks in Face B and Face D corresponding flange wall in X direction appear.

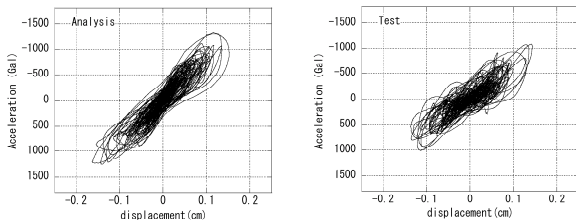
As for the RUN-4 excitation, maximum horizontal deflection angle in Y-direction reach 0.21cm(2.1/1000 rad), exceeding that in X-direction. This causes shear cracks are spread on all faces of walls. In the analysis Case B4, maximum horizontal deflection in Y-direction reach 0.25cm(2.5/1000 rad), exceeding that in X-direction. Shear cracks in Face B and Face D corresponding web wall in Y direction are generated and cracks are spread on all faces of walls.



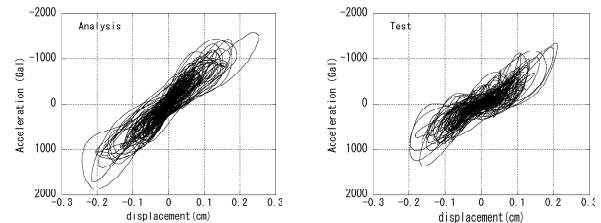
(X-direction)



(X-direction)



(Y-direction)



(Y-direction)

Figure 15 Hysteresis loop (CaseB3, RUN-3')

Figure 16 Hysteresis loop (CaseB3, RUN-4)

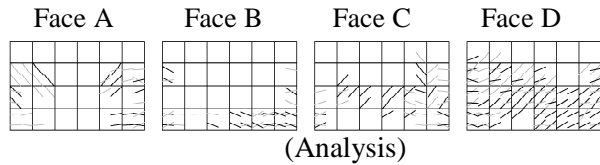


Figure 17 Crack pattern (Case B3, RUN-3')

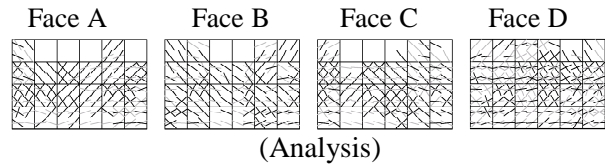


Figure 18 Crack pattern (Case B3, RUN-4)

Figure 19 shows comparison of hysteresis loops in Case B4 (RUN-7). Figure 20 shows crack patterns in Case B4 (RUN-7). Active and dormant cracks beyond 1500 μ are shown in analysis result. Yellow hatching portion shows failure.

On the RUN-7 excitation, the specimen reaches failure. Judging from hysteresis loops, deformation in Y-direction is saturated first and it is thought that failure of web wall in Y-direction is proceeding to that in X-direction. In the analysis, elements of bottom of face B and face D reach failure first, also more elements failed in faces B and D than the other faces A and C.

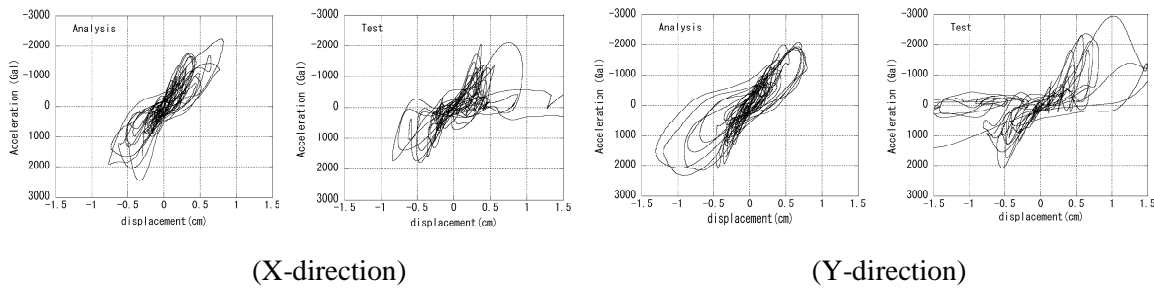


Figure 19 Hysteresis loop (Case B4, RUN-7)

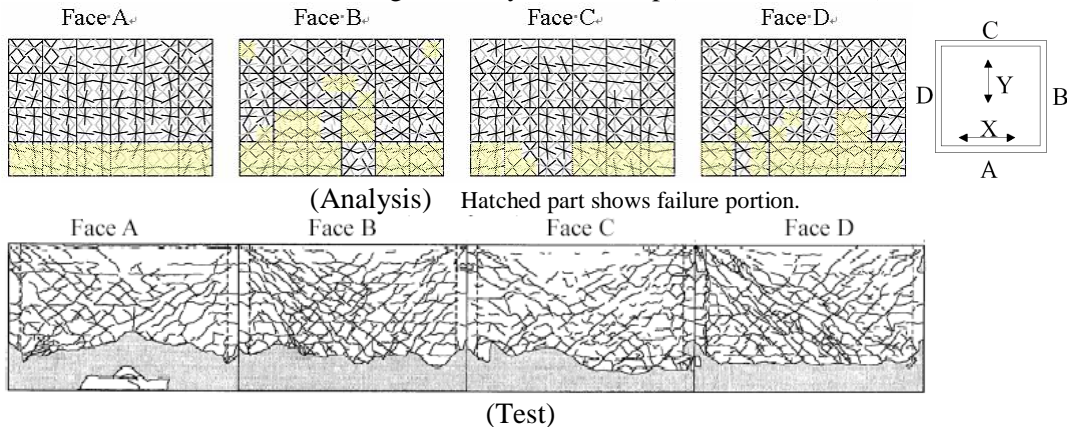
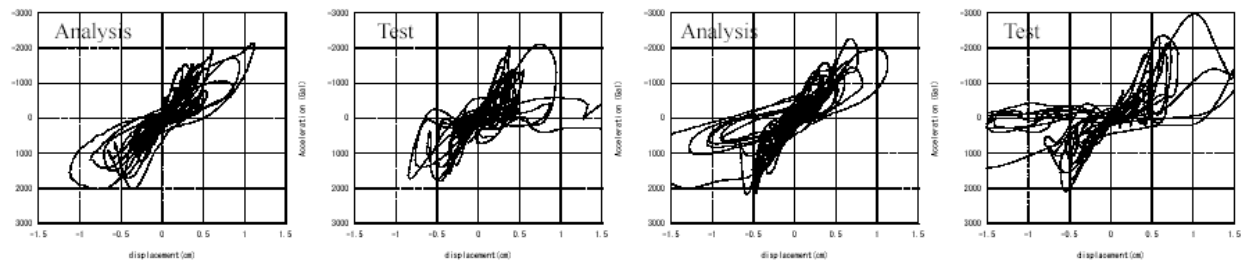


Figure 20 Crack pattern (Case B4, RUN-7)

Case B5 (large amplitude excitation, damping factor of 1%)

Figure 21 shows comparison of hysteresis loops in Case B5 (RUN-7). These results with damping factor of 1% give better agreement than results of case B4 with damping factor of 3%.

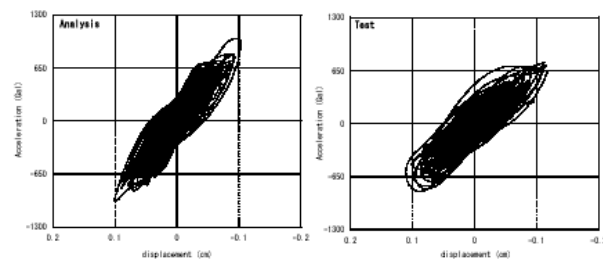


(X-direction) (Y-direction)
Figure 21 Hysteresis loop (Case B5, RUN-7)

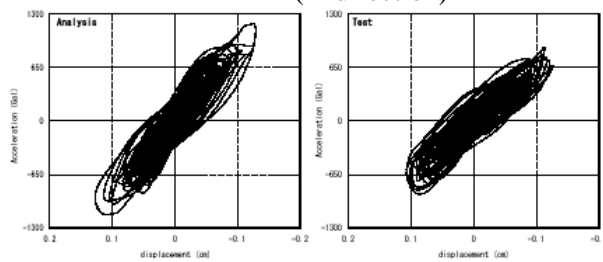
Case C1 (cylindrical wall, damping factor of 3%)

Figure 22 and 23 show comparison of hysteresis loops in CaseC1 (RUN-4 and RUN-5’).

On the RUN-4 excitation, maximum acceleration and horizontal (Y-direction) deflection reach 890 Gal and 0.13cm(1.3/1000 rad), respectively. On the RUN-5’ excitation, maximum acceleration and horizontal (Y-direction) deflection reach 1800 Gal and 0.30cm(3.0/1000 rad). These Hysteresis loops show S-shape, which is typical feature in case of strong nonlinearity of RC wall. Acceleration and deflection of analysis results show a little larger than those of test results. It seems that hysteresis loop of analysis results is S-shape as observed in test results. That tendency is similar with results of case B3 (box type wall).

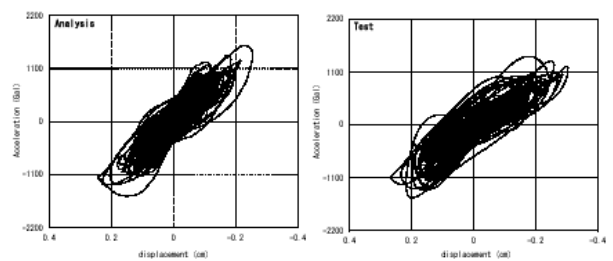


(X-direction)

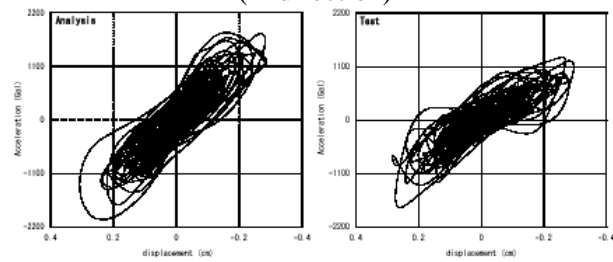


(Y-direction)

Figure 22 Hysteresis loop (Case C1, RUN-4)



(X-direction)



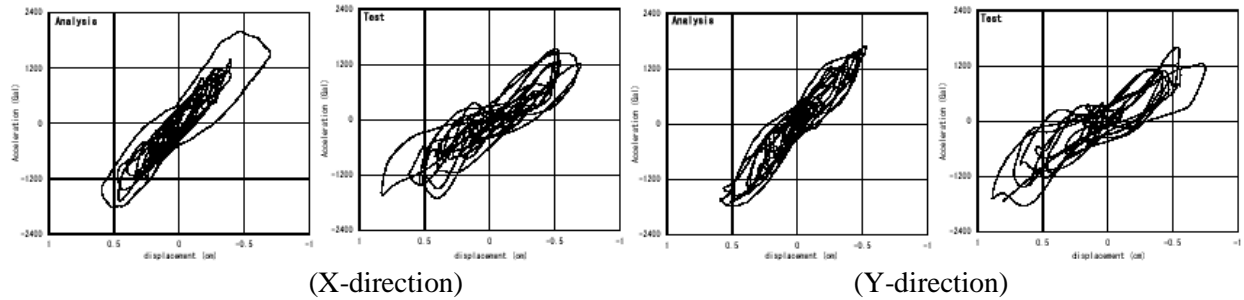
(Y-direction)

Figure 23 Hysteresis loop(Case C1, RUN-5’)

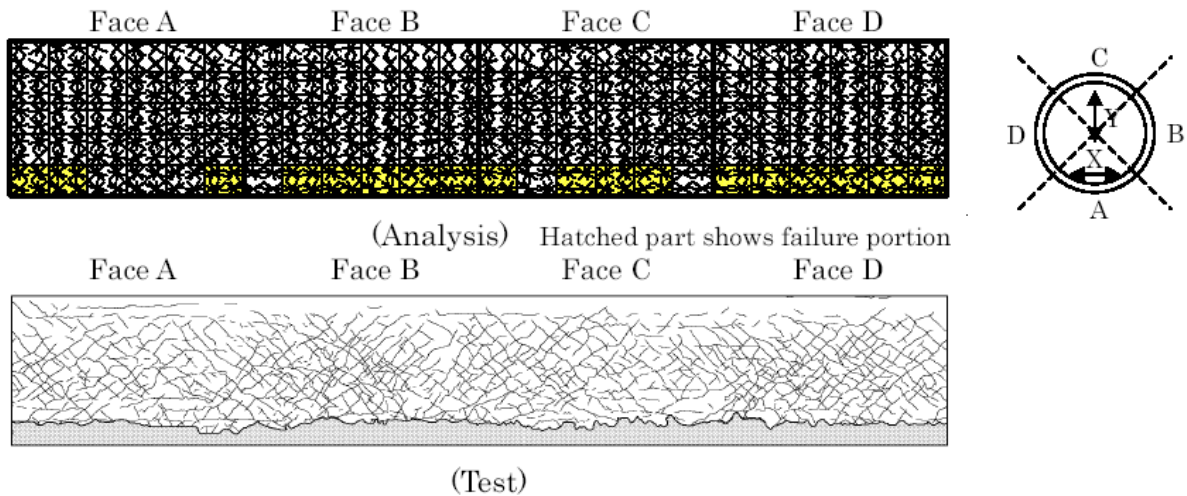
Case C2 (cylindrical wall, damping factor of 1%)

Figure 24 shows comparison of hysteresis loops in Case C2 (RUN-7). Deflection of analysis results shows a little smaller than that of test results.

Figure 25 shows crack patterns in Case C2 (RUN-7). Active and dormant cracks beyond 1500μ are shown in analysis result. Yellow hatching portion shows failure. Failure elements of analysis give good agreement with the test result.



(X-direction) (Y-direction)
 Figure 24 Hysteresis loop(Case C2, RUN-7)



(Analysis) Hatched part shows failure portion
 (Test)
 Figure 25 Crack pattern (Case C2, RUN-7)

CONCLUDING REMARKS

Simulation analysis of Box type and cylindrical RC shear wall specimens subjected to multi-directional dynamic input motions were conducted to study and to improve nonlinear FEM analysis method to evaluate seismic response from elastic range up to failure of RC structure with multi-directional input motions.

The results of the simulation analysis will be used to improve seismic safety analysis codes relevant to multi directional inputs and will contribute to improve the method of evaluating safety of nuclear power plant buildings.

ACKNOWLEDGEMENTS

This work was performed by NUPEC and JNES as a part of the "Model Test of Multi-axis Loading on RC Shear Walls" project commissioned by the Ministry of Economy, Trade and Industry (METI) of Japan. Technical issues have been discussed in the advisory committee on the project established by NUPEC (Chairperson: Professor Dr. T.Nishikawa). The authors wish to express their thanks to all the members of the committee for their valuable suggestions and co-operation.

REFERENCES

- 1 Kitada, Y., Torita, H., Matsumoto, R., Mihara, Y. and Nishikawa, T., "Shaking Table Test of RC Box-type Shear Wall in Multi-Axes Loading", Transactions of the 17th SMIRT, 2003.

- 2 Haruhiko Torita, Ryoichiro Matsumoto, Yoshio Kitada, Kazuhiro Kusama, and Takao Nishikawa, "SHAKING TABLE TEST OF RC BOX-TYPE SHEAR WALL IN MULTI-AXES LOADING ", 13th WCEE, 2004
- 3 Nuclear Power Engineering Corporation., "Report on Model Test of Multi-axis Loading on RC Shear Walls (In Japanese) ", March 2000.